Dependence of Acoustic Trapping Capability on the Orientation and Shape of Particles

Yanyan Liu, Junhui Hu, *Senior Member, IEEE*, and Chunsheng Zhao

***Abstract*—This paper presents an experimental and theoretical investigation of the dependence of acoustic trapping capability on the orientation and shape of particles to be trapped in different media. In the experimental investigation, two sharp edges of metal strips in ultrasonic vibration are used to trap particles in air. Experimental particles are made of clay, having the same mass and volume but different shapes. In the theoretical investigation, a method which combines the analysis of finite element method and theory of acoustic radiation force is used to calculate the acoustic radiation force acting on particles with different shapes and orientations. Both the experimental and theoretical results show that the acoustic trapping capability depends on the orientation and shape of particles. It is found that both in air and in water, for a particle with a given shape, the trapping capability is different at different orientations; for some commonly shaped particles, such as rectangular cuboid, cylinder, cone, cube, sphere, and hollow cylinder; the trapping capability for each particle shape at its best trapping orientation decreases in the listed sequence of shapes.**

I. Introduction

The acoustic radiation pressure is the unidirectional pressure on an object in a sound field, which is directly caused by sound and not related to acoustic streaming [1], [2]. The acoustic radiation force is the force caused by the acoustic radiation pressure. The theory of acoustic radiation force on an object in a sound field has been studied by many authors until the present day. King presented a detailed theoretical understanding of acoustic forces for a rigid sphere in plane standing or progressive wave fields in ideal fluid [3]. Embleton extended King's approach to the case of a rigid sphere in progressive spherical wave field [4]. Yosioka and Kawasima extended King's method to include the effects of a compressible sphere [5]. Using a different approach than King, Gor'kov used the far-field scattering method to calculate the force acting on a sphere in a sound field in ideal fluid [6]. Nyborg derived a simple expression of acoustic forces by extending the methods of King and Embleton [7]. Hasegawa and Yosioka calculated the acoustic radiation force on an elastic solid sphere suspended freely in a plane progressive sound field [8]. Barmatz and Collas applied the method of Gor'kov to derive the expressions of acoustic radiation potential and force on a sphere in plane, cylindrical, and spherical standing wave fields [9]. Marston derived an expression for the radiation force on a sphere placed on the axis of an ideal acoustic Bessel beam propagating in an inviscid fluid [10]. Besides these studies of the force on a spherical object in sound field, there are some researches into the acoustic radiation force on a cylinder. Awatani [11] and Hasegawa *et al.* [12] derived numerical results for acoustic radiation forces on rigid and elastic cylinders in plane progressive sound field, respectively. Wu *et al.* derived a simple and general analytical expression of acoustic radiation force on a rigid cylinder in standing wave field [13]. Wei *et al.* derived a method of acoustic radiation force on a compressible cylinder in standing wave field [14]. Mitri derived the exact expressions of acoustic radiation force on elastic, viscoelastic, and rigid cylinders in a standing wave field or quasi-standing wave field [15]–[17]. There are also a few works investigating the acoustic radiation force on some other types of objects, such as disks, spherical shells, bubbles, and so on [18]–[25]. Other significant works on acoustic radiation force are reported in [26]–[32].

The acoustic radiation force generated in the sound field can be used to manipulate particles, such as to collect, concentrate, separate, and transport particles. Particle manipulation by ultrasound has potential applications in household appliances, pharmaceutical production line, waste gas control, etc. Many particle manipulation techniques by ultrasound have been developed over decades. Coakley *et al.* investigated the cell manipulation in ultrasonic standing wave field [33]. Wu proposed acoustic tweezers using two collimated focused ultrasonic beams, in which the acoustic tweezers can trap latex particles of 270 μm diameter and clusters of frog eggs [34]. Takeuchi *et al.* developed a VHF-range leaky wave transducer to trap and transport 50-μm-diameter glass spheres in water [35]. Hu proposed a series of ultrasonic transducers to collect small plant seeds by acoustic radiation surface, such as π-shaped ultrasonic tweezers, a tapered aluminum strip, and others [36]–[38]. Other significant works in this area are reported in references [39]–[46].

Studying the above listed researches, it is found that all of them use the acoustic radiation force on a sphere or cylinder in plane standing and traveling wave fields. There has been no systematic work reported on the dependence of acoustic trapping capability on the orientation and shape of objects in complicated sound fields, such as the one near the radiation surface. In practical applications, objects have various shapes and can be in many orientations. In the applications, such as removing particles from a solid surface and separating particles from a mixture, it is necessary to understand the effects of particle shape and orientation on the trapping capability for the particle.

Manuscript received August 18, 2009; accepted February 21, 2010.

Y. Liu is with the School of Electrical and Electronics Engineering, Nanyang Technological University, Singapore.

J. Hu and C. Zhao are with the Laboratory of Precision Drive, Nanjing University of Aeronautics and Astronautics, Nanjing, China (e-mail: ejhhu@ntu.edu.sg).

Digital Object Identifier 10.1109/TUFFC.2010.1563

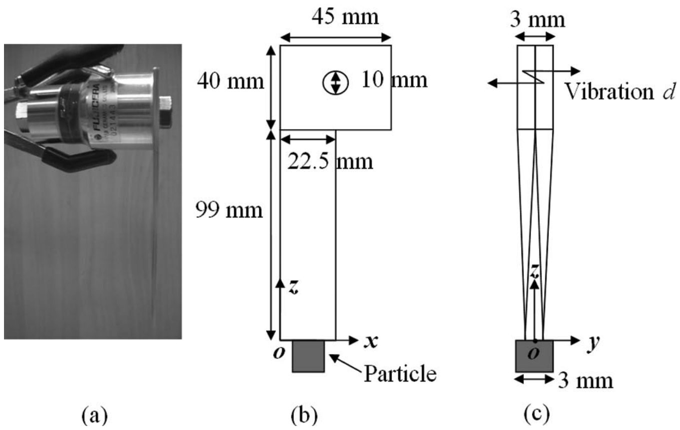

Fig. 1. Structure and size of the ultrasonic transducer with two V-shaped aluminum strips in air. (a) Photo of structure of the ultrasonic transducer. (b) Shape and size of the aluminum strip. (c) Air gap formed by the two V-shaped strips.

In this work, the effects of the orientation and shape of particles on the acoustic trapping capability for them have been investigated both experimentally and theoretically. In the experiment, two sharp edges of metal strips in ultrasonic vibration are used to trap particles in air. A method which combines the analysis of finite element method (FEM) and theory of acoustic radiation force is used to calculate the acoustic radiation force on various shaped particles in a complicated sound field. It is found that the acoustic trapping capability depends on the orientation and shape of the particles. The dependence of acoustic trapping capability on the orientation and shape of some commonly seen particles such as rectangular cuboid, cylinder, cone, cube, sphere, and hollow cylinder in different media is clarified experimentally and theoretically.

II. Experimental Setup and Analysis Method

The structure of transducer used to trap particles in air in the experiment is shown in Fig. 1, which has been reported in our previous work [47]. In this transducer, two identical aluminum strips are clamped to a Langevin transducer (FBL28452HS, Fuji Ceramics, Tokyo, Japan) as shown in Fig. 1(a). The aluminum strips have the shape and size shown in Fig. 1(b) and (c). The upper part of them is a rectangular aluminum plate, and the lower part is a V-shaped aluminum strip. The upper part has a size of 40 × 45 × 1.5 mm with a 10-mm-diameter hole at its center; the lower part with a length of 99 mm, width of 22.5 mm and thickness of 1.5 mm, is tapered off from the upper end to the lower end; the thickness of strip at the tip is around 200 µm. In this way, a triangular air gap is formed between the two V-shaped strips, which has a thickness of 1.3 mm at the tip. The Langevin transducer has a resonance frequency of 25.3 kHz. The 2-D FEM analysis by the acoustic module of COMSOL Multiphysics (Comsol Inc., Burlington, MA) shows that a flexural vibration is excited in the aluminum strips when an AC voltage with a frequency close to the resonance frequency of the ultrasonic transducer is applied. This flexural vibration will generate a sound field, and the sound field near the lower end of the gap can generate an acoustic radiation force to suck the particles to the lower end of strips [47].

The acoustic radiation force $\boldsymbol{F}$ on a rigid immovable object in a sound field in ideal fluid is given by the following integration over the surface of the object [2].

$$\boldsymbol{F} = \left\langle \iint_S (K - U)\boldsymbol{n}\, \mathrm{d}S \right\rangle, \tag{1}$$

where the notation $\langle\ \rangle$ denotes time average over one period, K is the kinetic energy density, U is the potential energy density, and $\boldsymbol{n}$ is the outward normal unit vector of the surface. The kinetic and potential energy densities K and U can be calculated by [2]

$$K = \frac{\rho_0 v^2}{2} \tag{2}$$

$$U = \frac{p^2}{2\rho_0 {c_0}^2}, \tag{3}$$

where ρ_0 and c_0 are the density of and sound speed in the fluid, v is the velocity, and p is the sound pressure.

The FEM analysis is conducted by the harmonic analysis of acoustic module of COMSOL Multiphysics for the sound field surrounding a particle under the two vibrating sharp edges in air as shown in Fig. 1(c) in 3-D. It is found that when the two identical metal strips are vibrating in the same y direction, the sound pressure in the air gap is antisymmetric about its central plane (xz-plane), therefore the sound pressure in the xz-plane is zero. Also it is found that the vibration velocity on particle surfaces is symmetric about the xz-plane. Because of the limitation of our 32-bit computer's addressable memory (physical RAM and disk swap space) for calculation, it is difficult to analyze the whole structure in 3-D, so we split the whole structure (two metal strips, a particle, and the surrounding sound field) into two parts about the xz-plane for the 3-D FEM calculation. The boundary conditions for the sound field are: $P = 0$ is used for the xz-plane; the rest of the sound field boundaries are radiation boundary. The excitation conditions for the transducer are: the excitation frequency f is 25.3 kHz, which is the resonance frequency of the transducer; the amplitude of the y-directional vibration displacement (0-peak) of the upper part of metal plates d is 10 µm; the loss factor of the vibration in aluminum is 0.02, which is defined as the ratio of the amount of energy dissipated as heat to that of total stored energy (COMSOL Multiphysics, Comsol Inc., Burlington, MA). Fig. 2(a) shows the mesh of the half structure (a single strip, half of a 3 × 3 × 3 mm cube particle and the surrounding sound field) in 3-D FEM calculation, where the maximum mesh size at the particle surface boundaries is around 0.66% of the wavelength. Figs. 2(b), (c), and (d)

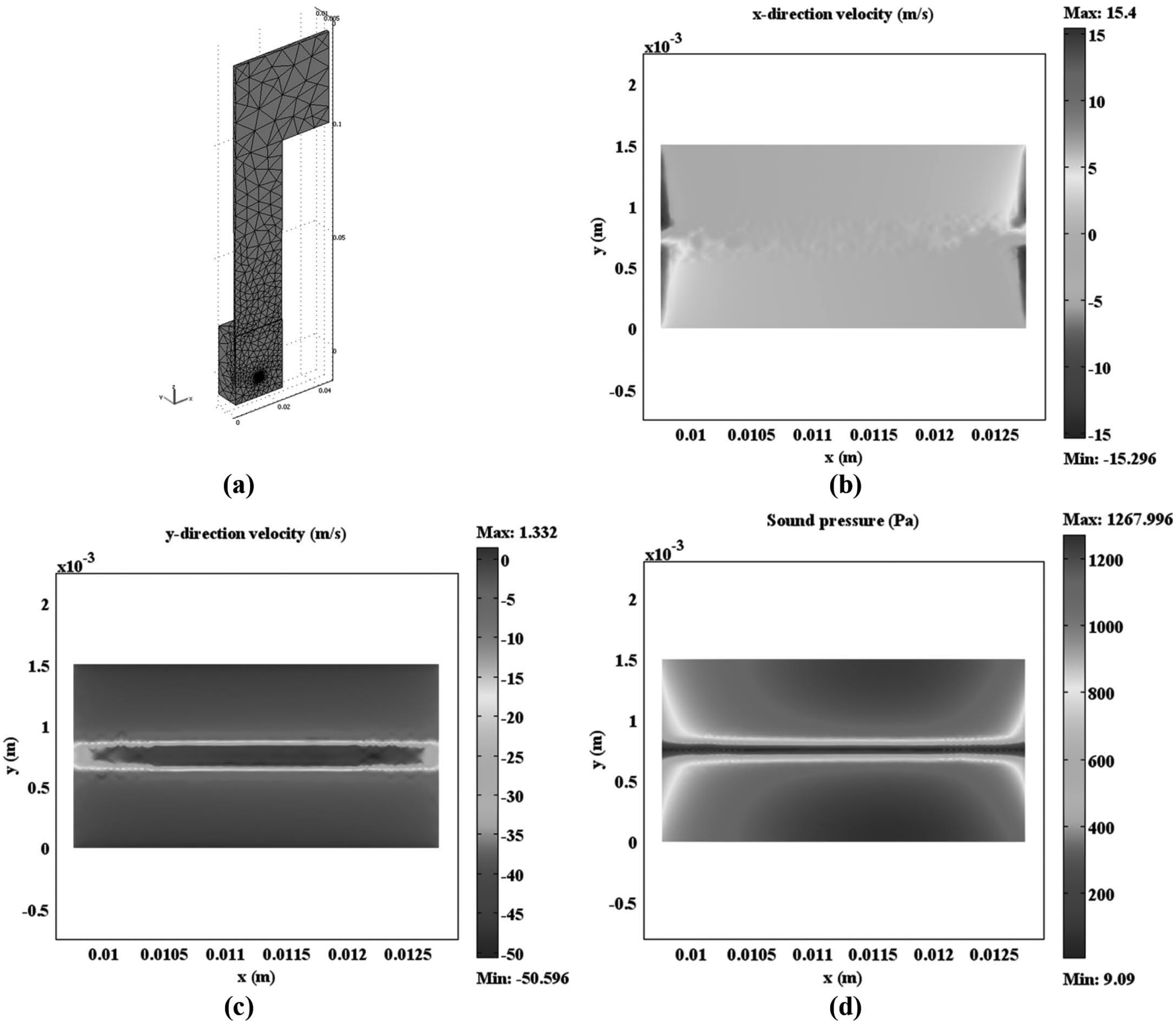

Fig. 2. 3-D FEM analyses of the half structure (a single strip, and half of a 3-mm-long cube particle and surrounding sound field) in air when a vibration displacement amplitude (0-peak) of upper part of metal plate is 10 µm. (a) Mesh. (b) The x-directional velocity on top surface of the half particle. (c) The y-directional velocity on top surface of the half particle. (d) The sound pressure on top surface of the half particle.

show the amplitudes of x-directional velocity, y-directional velocity and sound pressure on the top surface of the half particle. The z-directional velocity on top surface of the half particle is around 10^{-15} m/s, which is much smaller than the x-directional and y-directional velocities, thus it is not listed. It is seen that the x-directional velocity is very small compared with the y-directional velocity; the y-directional velocity is maximum at around $y = 0.75$ mm, which is near the sharp edge of the vibrating strip. From the 3-D FEM results shown in Fig. 2(b), (c) and (d), it is known that $\iint_S \langle K \rangle \mathrm{d}S$ and $\iint_S \langle U \rangle \mathrm{d}S$ on the top surface of the cube particle are calculated to be 6.5×10^{-4} N and 1.2×10^{-5} N, respectively. Also, it is found that $\iint_S \langle K \rangle \mathrm{d}S$ and $\iint_S \langle U \rangle \mathrm{d}S$ on the side and bottom surfaces of the particle are less than 1% of that on the top surface; thus, they are negligible. From the calculation, it is known that on the top surface of particle, $\iint_S \langle K \rangle \mathrm{d}S \gg \iint_S \langle U \rangle \mathrm{d}S$, so $\boldsymbol{F}$ has the same direction as $\boldsymbol{n}$ [see (1)], and the particle may be sucked to the sharp edge of the strips. Therefore, for the transducer used in our experiment, the acoustic radiation force acting on a particle is determined by the force on the top surface of the particle, pointing upwards; and the trapping force mainly occurs near the two vibrating sharp edges of the strips. Also, based on our FEM analysis, it is known that the negative acoustic radiation pressure is much larger in the contact area between the sharp edges of strips and top surface of particle than that at the other locations of the particle. So the x-directional length of the contact area is defined as the action line of the particle.

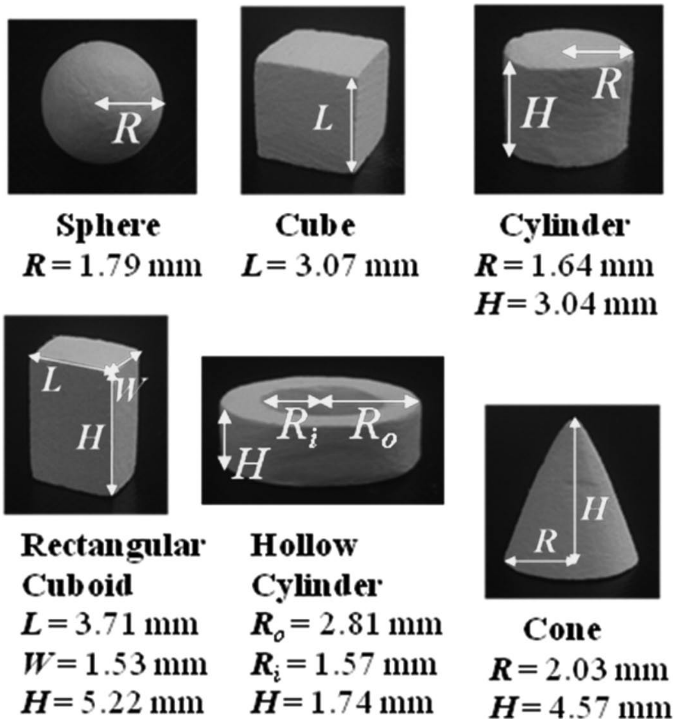

Fig. 3. Photos and dimensions of six different shaped clay particles with the same mass and volume.

Particles used in the experiment are made of clay. The sound speed of clay material is measured by a sound speed meter (SV-DH-7A, Guotai Electronics, Xi'an, China). In the method used, two cylindrical clay samples with different lengths (L_1 and L_2, respectively) are used, and the time for sound to travel through each sample in its length direction is measured (t_1 and t_2, respectively). The sound speed in clay material is calculated by the length difference ($\Delta L = L_1 - L_2$) and the time difference ($\Delta t = t_1 - t_2$), and the measured sound speed was found to be 2716 m/s. The density of clay material is calculated by using the measured mass and volume of clay particle, and the measured density is 1554 kg/m^3. There are six types of particles with different shapes but the same masses and volumes. The mass of each particle is 40 mg. The shapes of the six particles are sphere, cube, cylinder, cone, rectangular cuboid, and hollow cylinder. The size of each particle is shown in Fig.3. In the experiment, the two vibrating sharp edges of strips are moved to the top surface of particle, and then the transducer is lifted up. It is found that all of the six particles can be trapped in air by the transducer operating at a proper vibration. For the comparison of acoustic trapping capability, the acoustic trapping capability coefficient C_{tr} is defined as

$$C_{\mathrm{tr}} = \frac{1}{d_{\min}}, \tag{4}$$

where $d_{\min}$ is the minimum vibration displacement at the tip of metal strip to trap one particle. The acoustic trapping capability for a particle is stronger for greater values of C_{tr}. Fig. 4 shows the trapped rectangular-cuboid-shaped particle under the two sharp edges of the strips in air.

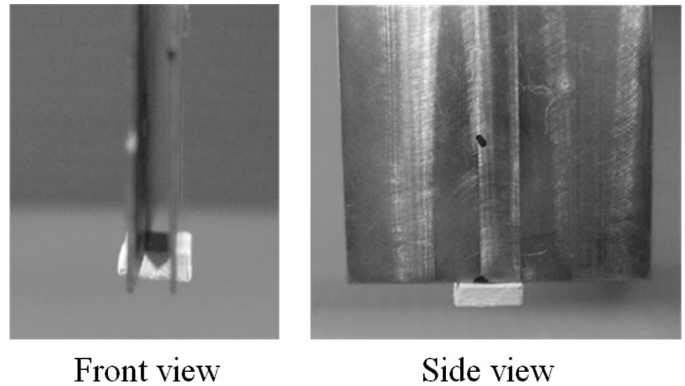

Fig. 4. A trapped rectangular cuboid shaped particle in air.

III. Results and Discussion

The effect of orientation of a rectangular cuboid particle on the acoustic trapping capability in air has been investigated both experimentally and theoretically. The rectangular cuboid particle trapped under the two sharp edges of metal strips has six possible trapping orientations, from ***a*** to ***f***, as shown in Fig. 5(a). Fig. 5(b) shows the experimental and calculated acoustic trapping capability coefficients for the rectangular cuboid particle at the different trapping orientations. In the experiment, the particle can be trapped at five orientations (***a***, ***b***, ***c***, ***d***, and ***e***), and experimental and calculated results agree well. Defining the contact line between the sharp edge of strip and the top surface of particle as the action line, the lengths of the action line of the rectangular cuboid particle from orientation ***a*** to ***f*** are 5.22, 5.22, 3.71, 3.71, 1.53, and 1.53 mm, respectively. It is found that the acoustic trapping capability coefficient C_{tr} increases mostly with the increase in the length of the action line. Also, with the same length of action line, a particle with larger top surface area [shaded area in Fig. 5(a)] has stronger acoustic trapping capability. For example, cases ***a*** and ***b*** have the same length of action line, but case ***a*** has larger trapping capability than case ***b***. This is because the larger the top surface area is, the larger is the action area of the upward acoustic radiation force.

Fig. 6 shows the experimental and calculated effects of the orientation of the cylindrical particle on the acoustic trapping capability in air. The cylinder particle has three possible trapping orientations, as shown in Fig. 6(a). From Fig. 6(b), it is seen that cylinder can be trapped at all the orientations; for orientation ***a*** and ***b***, the experimental and calculated results agree well; for orientation ***c***, the difference between the experimental and calculated results is relatively large. It is known that the length of the action line of cylinder particle for orientation ***c*** is 0 mm. The error in case ***c*** may be because a very short action line of a particle needs a finer mesh to reduce the calculation error and this requires a quite large memory for calculation. This is not easy to achieve with our current computer.

The acoustic trapping capability for particles in air with different shapes (as shown in Fig. 3) has been inves-

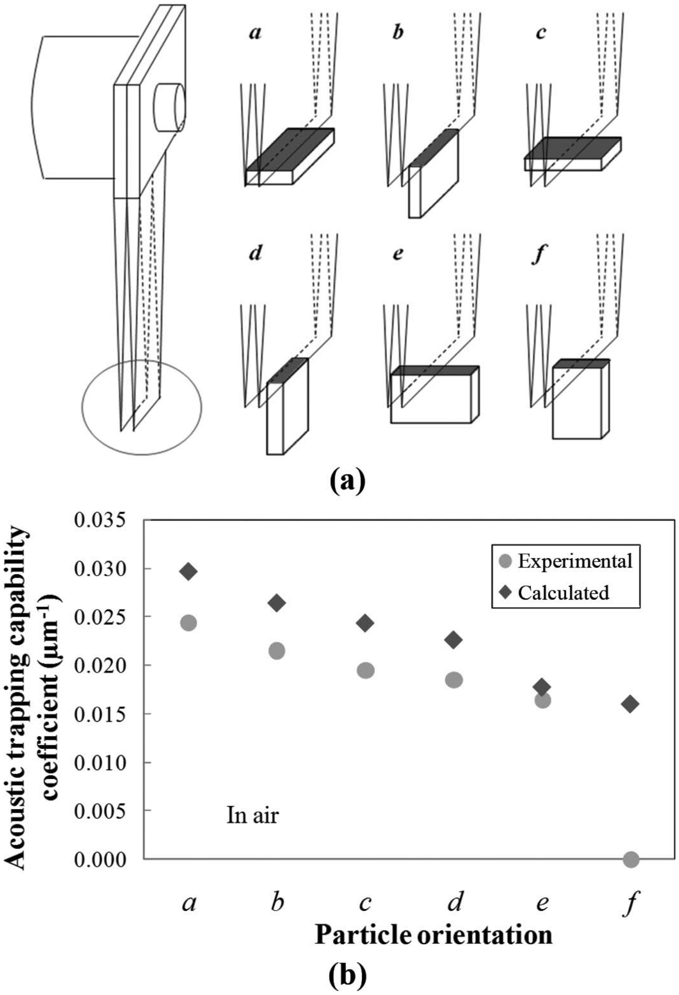

Fig. 5. The effect of orientation of rectangular cuboid clay particle on the acoustic trapping capability in air. (a) Six possible trapping orientations of the same rectangular cuboid shaped particle. (b) The experimental and calculated acoustic trapping capability coefficients for the rectangular cuboid particle at different trapping orientations.

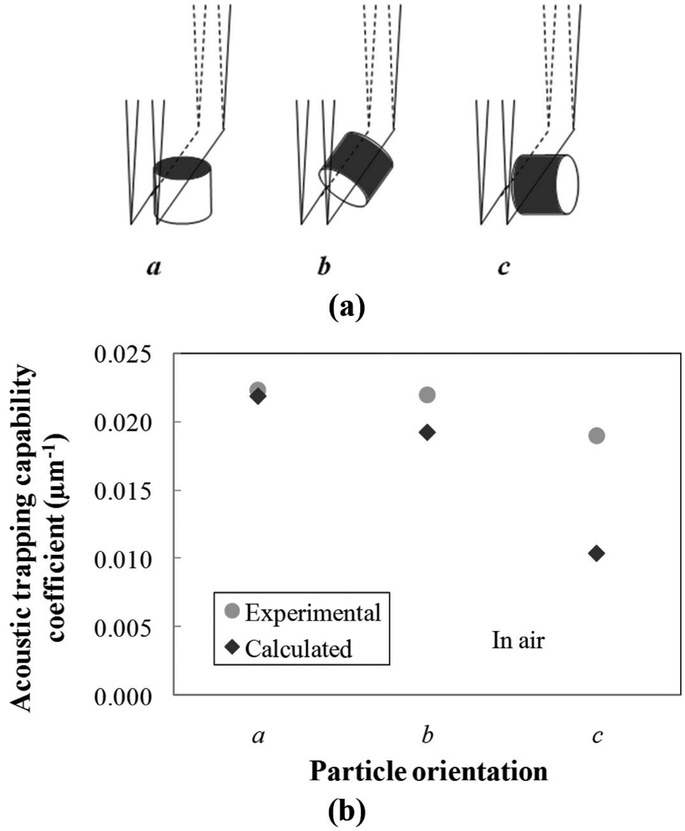

Fig. 6. The effect of orientation of cylinder clay particle on the acoustic trapping capability in air. (a) Three possible trapping orientations of the same cylinder shaped particle. (b) The experimental and calculated acoustic trapping capability coefficients for the cylinder particle at different trapping orientations.

tigated experimentally. For each particular particle shape, there are several possible trapping orientations, and every orientation has its own trapping capability. The best experimental trapping capability for each particle is used, as shown in Fig. 7(a). Fig. 7(b) shows the experimental and calculated acoustic trapping capabilities for particles with different shapes. The experimental acoustic trapping capability was found to be greatest to least for the particle shapes rectangular cuboid, cylinder, cone, cube, sphere, and hollow cylinder. The error between the experimental and calculated results is small except for the sphere and hollow cylinder. The theoretical calculations are not given for the sphere and hollow cylinder for the reason given in the discussion of Fig. 6.

The effect of orientation of the same rectangular cuboid particle on the acoustic radiation force acting on particle in water and in air is investigated theoretically, and the results are shown in Fig. 8. In the calculation, the vibration excitation conditions in water are the same as that in air ($d = 10$ μm and $f = 25.3$ kHz). The trapping orientations of the rectangular cuboid particle shown in Fig. 5(a) are used. From Fig. 8, it is seen that the acoustic radiation force acting on the rectangular cuboid particle decreases from orientation ***a*** to ***f*** both in air and in water; the acoustic radiation force on the particle in water is larger than that in air for the same particle at same orientation, because of the stronger sound field in water. Considering the buoyancy force on the particle in water, the trapping capability in water would be much stronger than that in air because the upward trapping force is enhanced by buoyancy force. In this analysis, the effect of acoustic streaming is not taken into account. It was experimentally found that there was no acoustic stream or the effect of acoustic stream on particle trapping was negligible when the vibration velocity was less than a critical value [25]. Our analysis is for the vibration range in which the effect of acoustic streaming is small.

Fig. 9 shows the calculated acoustic radiation forces acting on particles both in water and in air for the particles shown in Fig. 3, which have different shapes but the same volume and density. In the calculation, the vibration excitation conditions in water are the same as that in air ($d = 10$ μm and $f = 25.3$ kHz). The trapping orientation of each particle is as shown in Fig. 7(a). From Fig. 9, it is seen that the acoustic radiation force in water decreases from rectangular cuboid, cylinder, cone, cube, sphere, to hollow cylinder, which is the same order as that in air.

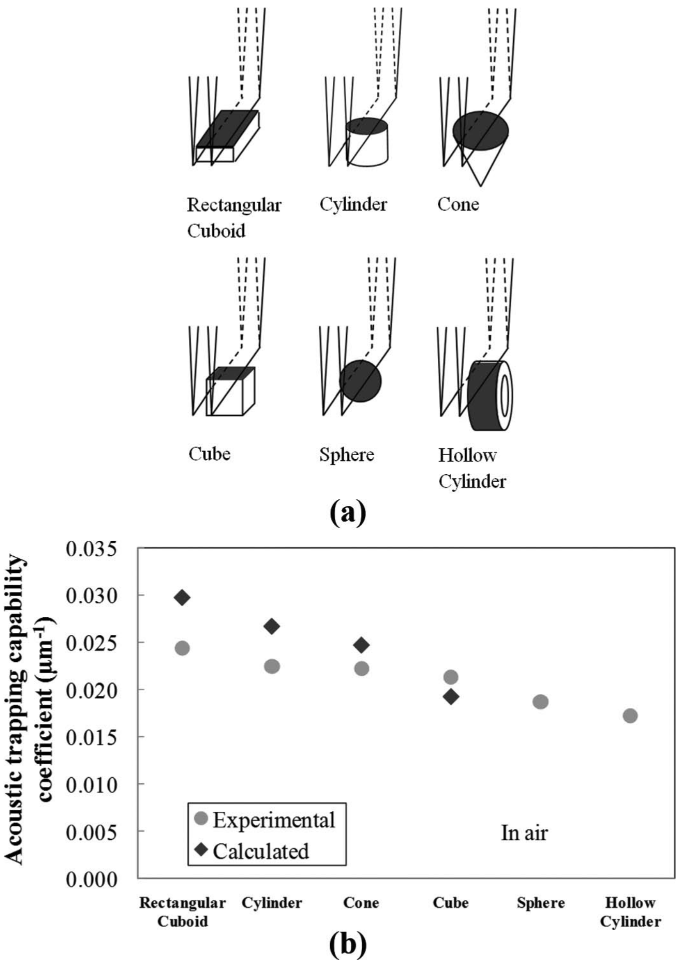

Fig. 7. The effect of particle shape on the acoustic trapping capability in air. (a) Six particles with different shapes but the same volume and density, at the orientation at which the experimental trapping capability is the strongest for each particle. (b) The experimental and calculated acoustic trapping capability coefficients for the particles at the orientations shown in (a).

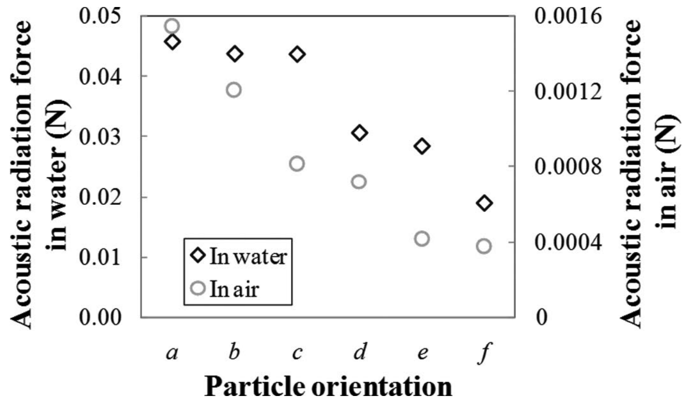

Fig. 8. The effect of orientation of the rectangular cuboid particle on the calculated acoustic radiation force acting on particle in water and in air.

Fig. 10 shows the calculated acoustic radiation force on rectangular cuboid particle at the interface of water and air. In the calculation, the vibration excitation conditions are the same as that in air and in water ($d = 10$ μm and $f = 25.3$ kHz); the trapping orientations of the rectangular cuboid particle shown in Fig. 5(a) are used, and half of the particle is in water and another half in air. From Fig. 10, it is seen that from orientation ***a*** to ***f***, the acoustic radiation force on particle at the interface of water and air decreases correspondingly. Compared with Fig. 8, it is found that the acoustic radiation force on particle at the interface of water and air is larger than that in air, and less than that in water.

IV. Conclusions

In summary, we have investigated the effects of orientation and shape of particles on the acoustic trapping capa-

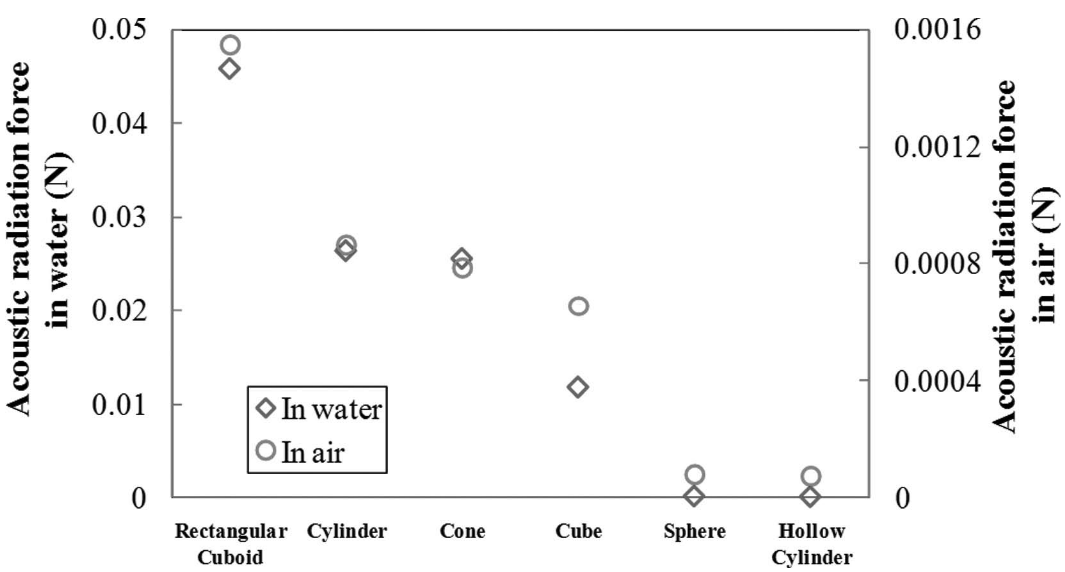

Fig. 9. The effect of particle shape on the calculated acoustic radiation force acting on particle in water and in air.

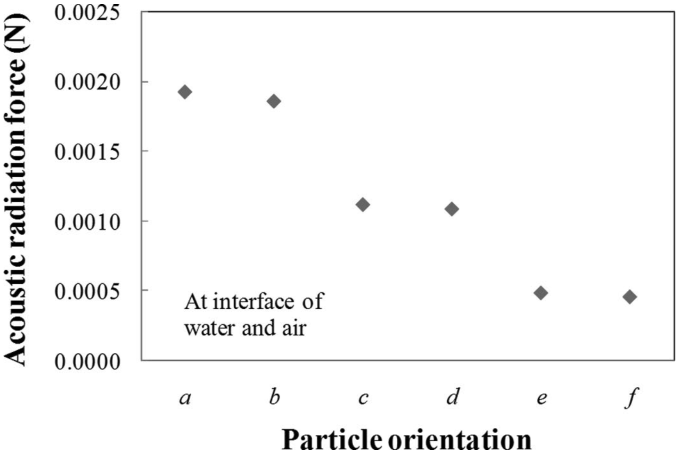

Fig. 10. The effect of orientation of the rectangular cuboid particle on the calculated acoustic radiation force when particle is at the interface of water and air.

bility in different media. When the density, volume, and mass per particle are constant, the acoustic trapping capability for particle depends on the orientation and shape of particle. This dependence is caused by the difference in the length of the action line of the acoustic radiation force acting on the particles. The acoustic trapping capability increases with the increase of the length of the action line. For a given particle, acoustic trapping capability is the best at the orientation where the action line is the longest. The acoustic trapping capability was found to be greatest to least for the particle shapes rectangular cuboid, cylinder, cone, cube, sphere, and hollow cylinder. A method which combines the FEM analysis and theory of acoustic radiation force was employed to calculate the acoustic radiation force acting on particles with various shapes and orientations. By comparing the experimental and calculated results, it is seen that this method can explain the experimental results well. Also it was found that the acoustic radiation force on a given particle is much larger in water than in air; the acoustic radiation force on particle at the interface of water and air is larger than that in air and less than that in water.

References

[1] C. L. Morfey, *Dictionary of Acoustics*. New York, NY: Academic Press, 2001, pp. 14–15.

[2] T. Hasegawa, T. Kido, T. Iizuka, and C. Matsuoka, "A general theory of Rayleigh and Langevin radiation pressures," *J. Acoust. Soc. Jpn. E*, vol. 21, no. 3, pp. 145–152, 2000.

[3] L. V. King, "On the acoustic radiation pressure on spheres," *Proc. R. Soc. Lond. A*, vol. 147, no. 861, pp. 212–240, 1934.

[4] T. F. W. Embleton, "Mean force on a sphere in a spherical sound field. I (Theoretical)," *J. Acoust. Soc. Am.*, vol. 26, no. 1, pp. 40–45, 1954.

[5] K. Yosioka and Y. Kawasima, "Acoustic radiation pressure on a compressible sphere," *Acustica*, vol. 5, pp. 167–173, 1955.

[6] L. P. Gor'kov, "On the forces on a small particle in an acoustical field in an ideal fluid," *Sov. Phys. Dokl.*, vol. 6, no. 9, pp. 773–775, 1962.

[7] W. L. Nyborg, "Radiation pressure on a small rigid sphere," *J. Acoust. Soc. Am.*, vol. 42, no. 5, pp. 947–952, 1967.

[8] T. Hasegawa and K. Yosioka, "Acoustic-radiation force on a solid elastic sphere," *J. Acoust. Soc. Am.*, vol. 46, no. 5B, pp. 1139–1143, 1969.

[9] M. Barmatz and P. Collas, "Acoustic radiation potential on a sphere in plane, cylindrical, and spherical standing wave fields," *J. Acoust. Soc. Am.*, vol. 77, no. 3, pp. 928–945, 1985.

[10] P. L. Marston, "Axial radiation force of a Bessel beam on a sphere and direction reversal of the force," *J. Acoust. Soc. Am.*, vol. 120, no. 6, pp. 3518–3524, 2006.

[11] J. Awatani, "Study on acoustic radiation pressure (VI): Radiation pressure on a cylinder," *J. Acoust. Soc. Jpn.*, vol. 9, no. 2, pp. 140–146, 1953.

[12] T. Hasegawa, K. Saka, N. Inoue, and K. Matsuzawa, "Acoustic radiation force experienced by a solid cylinder in a plane progressive sound field," *J. Acoust. Soc. Am.*, vol. 83, no. 5, pp. 1770–1775, 1988.

[13] J. Wu and G. Du, "Acoustic radiation pressure on a rigid cylinder: An analytical theory and experiments," *J. Acoust. Soc. Am.*, vol. 87, no. 2, pp. 581–586, 1990.

[14] W. Wei, D. B. Thiessen, and P. L. Marston, "Acoustic radiation force on a compressible cylinder in a standing wave," *J. Acoust. Soc. Am.*, vol. 116, no. 1, pp. 201–208, 2004.

[15] F. G. Mitri, "Theoretical and experimental determination of the acoustic radiation force acting on an elastic cylinder in a plane progressive wave—Far-field derivation approach," *N. J. Phys.*, vol. 8, no. 8, art. no. 138, 2006.

[16] F. G. Mitri, "Theoretical calculation of the acoustic radiation force acting on elastic and viscoelastic cylinders placed in a plane standing or quasistanding wave field," *Eur. Phys. J. B*, vol. 44, no. 1, pp. 71–78, 2005.

[17] F. G. Mitri, "Theoretical calculation of the modulated acoustic radiation force on spheres and cylinders in a standing plane wave-field," *Physica D*, vol. 212, no. 1–2, pp. 66–81, 2005.

[18] M. Kotani, "An acoustical problem relating to the theory of Rayleigh disc," *Proc. Phys.-Math. Soc. Jpn.*, vol. 15, pp. 30–57, 1933.

[19] L. V. King, "On the acoustic radiation pressure on circular discs: Inertia and diffraction corrections," *Proc. R. Soc. Lond. A*, vol. 153, no. 878, pp. 1–16, 1935.

[20] J. Awatani, "Studies on acoustic radiation pressure. II. (Radiation pressure on a circular disk)," *J. Acoust. Soc. Am.*, vol. 27, no. 2, pp. 282–286, 1955.

[21] J. Wu, "Calculation of acoustic radiation force generated by focused beams using the ray acoustics approach," *J. Acoust. Soc. Am.*, vol. 97, no. 5, pp. 2747–2750, 1995.

[22] A. Eller, "Force on a bubble in a standing acoustic wave," *J. Acoust. Soc. Am.*, vol. 43, no. 1, pp. 170–171, 1968.

[23] M. A. H. Weiser, R. E. Apfel, and A. E. Neppiras, "Interparticle forces on red-cells in a standing wave field," *Acustica*, vol. 56, pp. 114–119, 1984.

[24] F. G. Mitri, "Acoustic radiation force acting on elastic and viscoelastic spherical shells placed in a plane standing wave field," *Ultrasonics*, vol. 43, no. 8, pp. 681–691, 2005.

[25] F. G. Mitri, "Acoustic radiation force on an air bubble and soft fluid spheres in ideal liquids: Example of a high-order Bessel beam of quasi-standing waves," *Eur. Phys. J. E*, vol. 28, no. 4, pp. 469–478, 2009.

[26] P. J. Westervelt, "Acoustic radiation pressure," *J. Acoust. Soc. Am.*, vol. 29, no. 1, pp. 26–29, 1957.

[27] H. Olsen, W. Romberg, and H. Wergeland, "Radiation force on bodies in a sound field," *J. Acoust. Soc. Am.*, vol. 30, no. 1, pp. 69–76, 1958.

[28] B. T. Chu and R. E. Apfel, "Acoustic radiation pressure produced by a beam of sound," *J. Acoust. Soc. Am.*, vol. 72, no. 6, pp. 1673–1687, 1982.

[29] F. G. Mitri and Z. E. A. Fellah, "New expressions for the radiation force function of spherical targets in stationary and quasi-stationary waves," *Arch. Appl. Mech.*, vol. 77, no. 1, pp. 1–9, 2007.

[30] F. G. Mitri, "Acoustic radiation force on a sphere in standing and quasi-standing zero-order Bessel beam tweezers," *Ann. Phys.*, vol. 323, no. 7, pp. 1604–1620, 2008.

[31] F. G. Mitri and Z. E. A. Fellah, "Theory of the acoustic radiation force exerted on a sphere by a standing and quasi-standing zero-order Bessel beam tweezers of variable half-cone angles," *IEEE Trans. Ultrason. Ferroelectr. Freq. Control*, vol. 55, no. 11, pp. 2469–2478, 2008.

[32] F. G. Mitri, "Langevin acoustic radiation force of a high-order Bessel beam on a rigid sphere," *IEEE Trans. Ultrason. Ferroelectr. Freq. Control*, vol. 56, no. 5, pp. 1059–1064, 2009.

[33] W. T. Coakley, D. W. Bardsley, M. A. Grundy, F. Zamani, and D. J. Clarke, "Cell manipulation in ultrasonic standing wave fields," *J. Chem. Technol. Biotechnol.*, vol. 44, no. 1, pp. 43–62, 1989.

[34] J. Wu, "Acoustic tweezers," *J. Acoust. Soc. Am.*, vol. 89, no. 5, pp. 2140–2143, 1991.

[35] M. Takeuchi, H. Abe, and K. Yamanouchi, "Ultrasonic micromanipulation of small particles in liquid using VHF-range leaky wave transducers," in *Proc. IEEE Ultrasonics Symp.*, 1994, vol. 1, pp. 607–610.

[36] J. Hu, J. Yang, and J. Xu, "Ultrasonic trapping of small particles by sharp edges vibrating in a flexural mode," *Appl. Phys. Lett.*, vol. 85, no. 24, pp. 6042–6044, 2004.

[37] J. Hu, J. Xu, J. Yang, and J. Du, "Ultrasonic collection of small particles by a tapered metal strip," *IEEE Trans. Ultrason. Ferroelectr. Freq. Control*, vol. 53, no. 3, pp. 571–578, 2006.

[38] J. Hu, J. Yang, J. Xu, and J. Du, "Extraction of biologic particles by pumping effect in a π-shaped ultrasonic actuator," *Ultrasonics*, vol. 45, no. 1–4, pp. 15–21, 2006.

[39] K. Yasuda, S. Umenura, and K. Takeda, "Concentration and fractionation of small particles in liquid by ultrasound," *Jpn. J. Appl. Phys.*, vol. 34, pt. 1, no. 5B, pp. 2715–2720, 1995.

[40] H. M. Hertz, "Standing-wave acoustic trap for nonintrusive positioning of microparticles," *J. Appl. Phys.*, vol. 78, no. 8, pp. 4845–4849, 1995.

[41] K. Ohtani, Y. Koike, S. Ueha, and H. Yokoi, "Novel wedge-shaped doubly inclined chamber for the flow-through separation of suspended particles," *Ultrasonics*, vol. 38, no. 1–8, pp. 647–649, 2000.

[42] M. Wiklund, S. Nilsson, and H. M. Hertz, "Ultrasonic trapping in capillaries for trace-amount biomedical analysis," *J. Appl. Phys.*, vol. 90, no. 1, pp. 421–426, 2001.

[43] A. Haake and J. Dual, "Contactless micromanipulation of small particles by an ultrasound field excited by a vibrating body," *J. Acoust. Soc. Am.*, vol. 117, no. 5, pp. 2752–2760, 2005.

[44] Y. H. Lee and C. A. Peng, "Enhanced retroviral gene delivery in ultrasonic standing wave fields," *Gene Ther.*, vol. 12, no. 7, pp. 625–633, 2005.

[45] M. K. Tan, J. R. Friend, and L. Y. Yeo, "Direct visualization of surface acoustic waves along substrates using smoke particles," *Appl. Phys. Lett.*, vol. 91, art. no. 224101, 2007.

[46] S. K. Chung and S. K. Cho, "On-chip manipulation of objects using mobile oscillating bubbles," *J. Micromech. Microeng.*, vol. 18, no. 12, art. no. 125024, 2008.

[47] Y. Liu and J. Hu, "Trapping of particles by the leakage of a standing wave ultrasonic field," *J. Appl. Phys.*, vol. 106, no. 3, art. no. 034903, 2009.

Yanyan Liu received the B.E. degree in electrical and electronic engineering from Nanyang Technological University (NTU), Singapore, in 2006. She has submitted her Ph.D. thesis to the School of Electrical and Electronic Engineering, NTU, Singapore in 2010. Her main research interests focus on ultrasonic and piezoelectric devices.

Junhui Hu received his Ph.D. degree from Tokyo Institute of Technology, Tokyo, Japan, in 1997, and B.E. and M.E. degrees in electrical engineering from Zhejiang University, Hangzhou, China, in 1986 and 1989, respectively. He is currently a Chang Jiang Scholar of the Ministry of Education of China, and a full professor at Nanjing University of Aeronautics and Astronautics, Nanjing, China.

Dr. Hu was a research engineer at the R&D Center of NEC-Tokin, Sendai, Japan, from November 1997 to February 1999, a research fellow and postdoctoral fellow at Hong Kong Polytechnic University, Hong Kong, China, from 1999 to 2001, an assistant professor at Nanyang Technological University, Singapore, from 2001 to 2005, and associate professor at the School of Electrical and Electronic Engineering, Nanyang Technological University, from 2005 to 2010. He was a research student at Yamagata University, Yonezawa, Japan, from October 1993 to March 1994. His present research interests include ultrasonic actuators and transducers, piezoelectric transformers and generators, physical effects of ultrasound, wireless drive of piezoelectric components, and novel applications of power ultrasound. Dr. Hu won the Paper Prize from the Institute of Electronics, Information and Communication Engineers (Japan) in 1998, and was awarded the title of valued reviewer of *Sensors and Actuators A* in 2009. He is the author and co-author of more than 100 papers and disclosed patents. He is a senior member of IEEE.

Chunsheng Zhao's photograph and biography were unavailable at time of publication.